Chiral Colloids: Homogeneous Suspension of Individualized SiO_2 Helical and Twisted Nanoribbons

Yutaka Okazaki,[†] Jiaji Cheng,[‡] Dmytro Dedovets,[‡,§] Gregor Kemper,[‡] Marie-Hélène Delville,[§] Marie-Christine Durrieu,[‡] Hirotaka Ihara,[†] Makoto Takafuji,[†] Emilie Pouget,[‡,*] and Reiko Oda[‡,*]

[†]Department of Applied Chemistry and Biochemistry, Kumamoto University, 2-39-1, Kurokami, Kumamoto 860-8555, Japan, [‡]Institute of Chemistry & Biology of Membranes & Nanoobjects (UMR5248 CBMN), CNRS, Université de Bordeaux, Institut Polytechnique Bordeaux, 2 rue Robert Escarpit, 33607 Pessac, France, and [§]Institut de Chimie de la Matière Condensée de Bordeaux (UPR9048 ICMCB), CNRS, 87 avenue du Dr. A. Schweitzer, F-33608 Pessac, France

ABSTRACT Finely tuned chiral nanometric silica fibers were synthesized based on sol–gel chemistry using organic self-assembly as a template. The optimization of the sol–gel process in acidic conditions allowed us to reduce the transcription time by a factor of 10. These nanohelices were successfully fragmented while preserving the fine internal structures from several micrometers to several hundreds of nanometers in length by a sonication method previously reported for carbon nanotubes. By carefully choosing the nature of the solvent, the sonication power, pH in the case of water, and densification of the silica walls by freeze-drying, the homogeneous and stable colloidal suspensions of individualized chiral nanometric silica ribbons with controlled length were obtained.

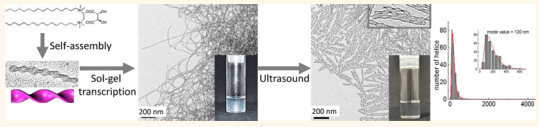

KEYWORDS: chiral nanostructures · chiral colloidal suspension · length control of nano-objects · sonication

In recent years, considerable progress has been made in the preparation of discrete nanostructures as nanoparticles or nanotubes with controllable chemical compositions and morphologies.[1−3] Nanorods, tubes, or platelets are particularly interesting due to their anisotropic properties.[4−11] Among them, those expressing chirality at the nanometer scale such as twisted or helical nanoribbons represent a new class of objects having an important potential in a large panel of applications due to their mechanical properties (helical nanoribbons can undergo a high elastic and reversible deformation), high specific surface area, electromagnetic properties, or optical chirality as described in a recent review by Wang *et al.*[12] Depending on the chemical compositions of the nano-objects and the nature of the functions grafted on their surface, these chiral nanostructures can be used in various functional devices and are studied for several applications such as catalysis,[13,14] nanosensors,[15] nanophotonics,[16,17] more generally nanoelectromechanical systems.[18]

Inspired by the template-directed sol–gel science,[19−21] researchers usually synthesize inorganic chiral objects using pre-existing organic chiral structures as templates.[22−27] These organic templates are often supramolecular self-assemblies based on directional interactions such as hydrogen bonding or π-stacking, and they express the chirality with helical (cylindrical curvature) or twisted (Gaussian curvature) geometries with well-defined periodicity, diameter, and handedness. In a majority of the cases, the handedness of these helices are directly linked with the stereochemistry of the components. The inorganic chiral fibers obtained by the replication of such structures reflect therefore the handedness of the organic templates. Meanwhile, reports on these nano-objects with *controllable* chiral morphology are rare because of the intrinsic difficulty encountered in the control of their synthesis.[22,28−31] Particularly, for most cases, the fibrous organic structures show an *uncontrolled* growth resulting in materials that consist of highly entangled fibers with knots, not suited for applications in functional materials. Indeed, for practical use, it is crucial to prepare individualized nanostructures with controlled length, orientation, and eventually hierarchical organization. Because ensembles of nanoparticles can have collective properties that are different from those displayed by individual ones or bulk samples, research activities in the field of nanoscience are shifting from synthesis of individual nanoparticles to the preparation of nanoparticle assemblies.[1,32] A number of

* Address correspondence to e.pouget@cbmn.u-bordeaux.fr, r.oda@cbmn.u-bordeaux.fr.

Received for review March 20, 2014 and accepted June 2, 2014.

Published online June 02, 2014
10.1021/nn501560w

works are reported on directed assemblies of spherical nanoparticles or nanorods. In most of the cases, stable colloidal solutions are needed as a starting point to induce such organization. To the best of our knowledge, only some chiral mesoporous silica are known to be of colloidal size with reproducible length and none forming stable colloidal solutions have been synthesized so far.[33,34] The only colloidal suspensions of chiral rod-like objects were obtained with organic particles, more particularly with biological structures which show a perfect morphological control like the fd virus or the tobacco mosaic virus.[35−39] This is why it turns out to be a real challenge to obtain stable suspensions of *individualized* chiral fibers with finely controlled morphology.

Previously, we reported the synthesis of nanometric helical and twisted silica ribbons with controlled handedness using organic assemblies of amphiphilic molecules as templates. The amphiphiles are cationic bis-quaternary ammonium gemini surfactants[40,41] with the following formula C_2H_4-1,2-$((CH_3)_2N^+C_{16}H_{33})_2$, with a tartrate counterion, denoted hereafter 16-2-16 tartrate.[42−44] With L- and D- tartrate counterions, they form right and left handed helices, respectively. The mixture of the two allowed us to continuously tune the twist pitches of these helices, making them the first examples of such continuous chirality variation. The relationship between the handedness, pitch, and circular dichroism signals was studied in detail.[45] The silica chiral ribbons synthesized from these organic templates reflect the handedness of the templates, where we could also perform the continuous control of the twist pitch of the silica helices.[46] Our study by three-dimensional tomography also unambiguously confirmed the handedness of these silica nanohelices; that is, silica from 16-2-16 L-tartrate forms right-handed helices and *vice versa* (Supporting Information Figure S1).[47] These silica structures were used as templates to generate hybrid nanostructures such as gold nanoparticle/silica helices for SERS substrates[47] or to create extracellular matrix mimetic materials to probe the cell−material interactions.[48] For these systems, the transcription of organic fibrous gels led to inorganic gel-like networks of chiral fibers.

In this report, we show how to fragment these entangled nano-objects in order to obtain individualized helical or twisted ribbons with controlled length. For this purpose, we were inspired by reports on the scission and suspension of carbon nanotubes *via* ultrasonication.[49−51] This technique when applied to an entangled metal oxide inorganic replica gave homogeneous colloidal dispersions of individualized helical or twisted ribbons. The impact of the sonication power on the helices' dispersion and the stability of the prepared suspensions studied in different solvents. Indeed, the stability of the colloidal suspension depends strongly on the balance of forces such as van der

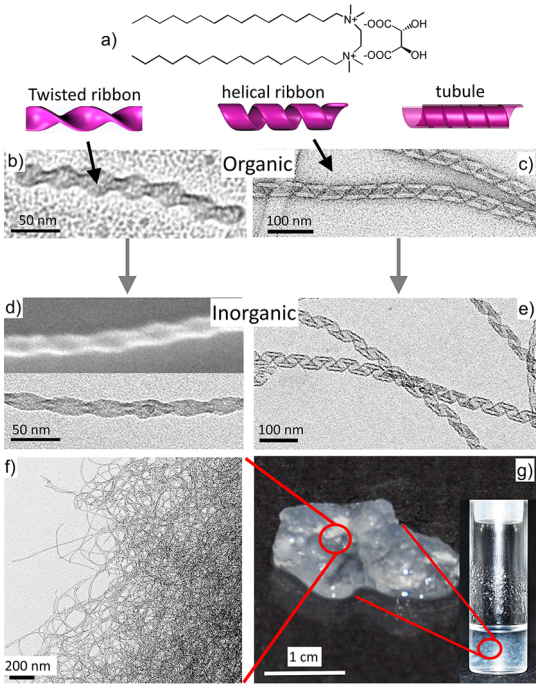

Figure 1. Sol−gel quick transcription of twisted and helical ribbons from self-assemblies of 16-2-16 tartrate. (a) Chemical formula of 16-2-16 tartrate, organic self-assembled (b) twisted ribbons and (c) helical ribbons. After the polycondensation of prehydrolyzed TEOS, silica (d) twisted and (e) helical nanoribbons are obtained. At a mesoscopic level, (f) they form an entangled 3D network, and macroscopically, (g) gel formation is observed.

Waals forces and electrostatic forces, thus the role of solvents is crucial. Such suspensions are extremely promising candidates for the preparation of hierarchically organized materials for functional devices as described above.

RESULTS AND DISCUSSION

As described in a previous paper,[22] the silica helical and twisted nanoribbons are synthesized through the inorganic transcription of self-assembly of cationic dimeric surfactants (gemini surfactants) with chiral tartrate counterions (Figure 1a). It is generally agreed in the literature that the chirality of organic helical or twisted ribbons based on molecular assemblies is intrinsic to the chirality of the constituent molecules. In the present case, the chirality of supramolecular fibers correlates to the chiral nature of the counterions. This gives rise to a facile control over the morphology of the organic molecular assemblies by the concentration and stoichiometric ratio of the counterions and the aging of the gel,[52] varying from flat ribbons, twisted ribbons (Figure 1b), and helical ribbons (Figure 1c) to nanotubes with various diameters, pitches, and handedness. With L-tartrate, right-handed helices are formed, whereas with D-tartrate, left-handed helices are observed. Figure 1 shows the different steps of the mineralization (transcription). First, organic helical or twisted nanoribbons are formed by the self-assembly of 16-2-16

TABLE 1. Time Required To Obtain Silica Twisted and Helical Ribbons Using TEOS Prehydrolyzed at pH 6.0 and pH 3.8

	prehydrolysis pH 6.0 for 12 h			prehydrolysis pH 3.8 for 7 h		
	organic aging	transcription time	timing for overall process	organic aging	transcription time	timing for overall process
helical ribbons	21 days	1.5 days	23 days	1—3 days	15 h	2—4 days
twisted ribbons	5 days	1.5 days	7 days	1—2 h	15 h	1 days

tartrate, then, a solution of prehydrolyzed tetraethoxysilane (TEOS) is mixed with these organic chiral ribbons where the polycondensation of silica occurs at the surface of the nanometric helical or twisted silica ribbons. In this paper, the term "helices" will be used as a general term to refer to helical and twisted silica nanoribbons at the same time.

Quick Transcription. In our previous paper, we reported that due to the competitive interaction of prehydrolyzed TEOS and chiral tartrate anions with the cationic surface of the fibers, the organic gels needed to be aged (consolidated) in order to keep the helical morphology after transcription.[22] To obtain twisted and helical silica ribbons, it took 7 and 23 days, respectively (Table 1). However, by modifying the pH of prehydrolysis of the TEOS with tartaric acid with the same enantiomer as that of the gemini counterion, and mixing it into organic helices, it is possible to considerably accelerate the inorganic transcription process and at the same time decrease the organic aging time without disturbing the helical morphology. By adding the tartaric acid, two phenomena take place: (i) on the one hand, the cationic charge of the surface of the ribbons is more screened and unfavorable for the condensation of anionic prehydrolyzed TEOS; (ii) on the other hand, the hydrolysis of TEOS is strongly accelerated at this pH; the latter over-riding the effect of the former. Here, it is important to use tartaric acid to adjust the pH, in order to not disturb the chiral environment at the organic helices' surface. With this method, twisted and helical silica ribbons (Figure 1d,e) were obtained within 1 and 3 days, respectively (Table 1).

In summary, with the new method, silica helical nanoribbons were obtained from 2 day aging instead of 21 day aging of the organic gel, and for twisted ribbons, 1—2 h aging (organic gel), instead of 5 days, was enough followed by 7 h prehydrolysis and 15 h transcription at pH 3.8 instead of 12 h prehydrolysis and 36 h transcription at pH 6.0. The optimized methods presented here allowed us to synthesize about 0.6 mg of silica helical ribbons and 1.1 mg of silica twisted ribbons from 0.36 mg of gemini 16-2-16 tartrate. It is important to note that the use of a roller-mixer while mixing the organic fibers and prehydrolyzed TEOS as described in the Experimental Section is crucial because it optimizes the contact of prehydrolyzed TEOS and organic fibers. Using this method, 50 mg of silica helices could be synthesized in one shot, pointing out the possible scaling up of this process.

In the procedure described above, we used tartaric acid with the same enantiomer as that of the gemini counterion in order to decrease the pH of TEOS suspension to accelerate their hydrolysis. In order to separately investigate the effect of pH and of the interfacial concentration of tartrate, we then performed the complementary experiments,

(1) lowering the pH using weak achiral acid, such as acetic acid, and
(2) prehydrolyzation of TEOS in the presence of 0.1 mM of sodium salt of tartrate, maintaining the pH at 6.

The results were very interesting.

(1) These experiments showed that in order to reach pH 3.8, 0.8 mM acetic acid (instead of 0.1 mM tartaric acid) was needed. This means that there is almost as much acetate ions as tartrate ions (the counterions of 16-2-16) when mixed with 1 mM 16-2-16 tartrate solution. In spite of that, silica helical ribbons with the identical pitch and diameters were obtained (Supporting Information). This indicated that the kinetics of morphology perturbation by the addition of an achiral acetate ion was slower than the acceleration of prehydrolyzation of TEOS and transcription in acidic conditions. This procedure led us to the average 0.26 mg of silica helical ribbons from 0.35 mg of gemini 16-2-16 tartrate.

(2) Surprisingly, we also obtained silica helices with the same pitch and diameter at pH 6 *in the presence of tartrate (0.1 mM)* after the fast fabrication procedure! Although the prehydrolysis of TEOS is slow at this pH, the presence of tartrate at the interfacial region of organic helix "protects" the chiral environment, thus the young gels (short aging time, *i.e.*, 2 days) remains helical during the transcription. This procedure led us to the average 0.34 mg of silica helical ribbons from 0.36 mg of gemini 16-2-16 tartrate.

These results show that the use of tartaric acid has both the effect of *lowering pH* (acceleration of TEOS prehydration) and the *presence of tartrate* (increase of interfacial tartrate concentration). While our results show that keeping only one of the two conditions seems sufficient for obtaining silica helical ribbons with a fast transcription procedure, the yields were less compared to when we used tartaric acid (about half, compared to 0.6 mg).

While the morphology of the final silica fibers (helical or twisted ribbons) is very well-controlled in terms of diameter, pitch, and handedness, these chiral fibers form knots and are entangled (Figure 1f),

resulting in a gel formation (Figure 1g). This causes problems for most of the potential applications which call for individualized chiral inorganic fibers. To achieve suspensions of such fibers, they have to be disentangled and fragmented in a controlled way.

A number of reports have shown how carbon nanotubes can be fragmented and suspended in solution when submitted to a strong sonication. It was observed that the effect of sonication on the dispersion and debundling of the carbon nanotubes strongly depended on the physical properties of the solvent, including viscosity, surface tension, density, molecular weight, and vapor pressure.[53] Inspired by these studies, we have developed a process to fragment and disperse the silica helical and twisted ribbons in different solvents. We optimized various parameters, in particular, the nature of the solvent, the sonication power, and the concentration of the suspension.

Effect of Solvents. The previous studies concerning the sonication effect on carbon nanotubes have shown that the nature of the solvent played an important role on their scission and dispersibility.[53] The high energy applied to the suspension during the sonication induces the formation, growth, and collapse of bubbles which create a depression, leading to the cavitation effect.[49,50] While imploding, the bubble can produce a shock wave able to break or disentangle the silica structures. The efficiency of the cavitation process is then closely correlated to solvent parameters such as vapor pressure, viscosity, and surface tension. Moreover, the stabilization of the suspension is also directly linked to the nature of the solvents. Therefore, we performed a systematic study of the scission and stabilization of the silica helices and ribbons in various solvents. For this study, parameters such as the silica fibers concentration (1 mg/mL), the volume (2 mL), sonication time (15 min), and power (130 W) were fixed and only the solvents in which the helices were sonicated were varied from ethanol by centrifugation and redispersion. We will refer to this method as "wet method" since the silica ribbons remain in solvents. Figure 2 shows the images of twisted nanoribbons after sonication in solvents which are miscible with water (ethanol, dimethyl sulfoxide (DMSO), dimethylformamide (DMF), acetonitrile, pyridine) and others which are not miscible with water (hexane and toluene).

The analysis of the TEM pictures shows that the nature of the solvent indeed plays a crucial role in the sonication process. In water (Figure 2a), the silica fibers are not fragmented or disentangled, but rather the high energy delivered when the cavitation bubbles implode induces the damage of the fine structure of the helices or twisted ribbons as is observed in the higher-resolution image (Figure 2a, inset). The damage is less pronounced in ethanol, but a strong aggregation is still observed (Figure 2b). On the other hand, in other solvents such as DMSO, DMF, or pyridine (Figure 2c–e)

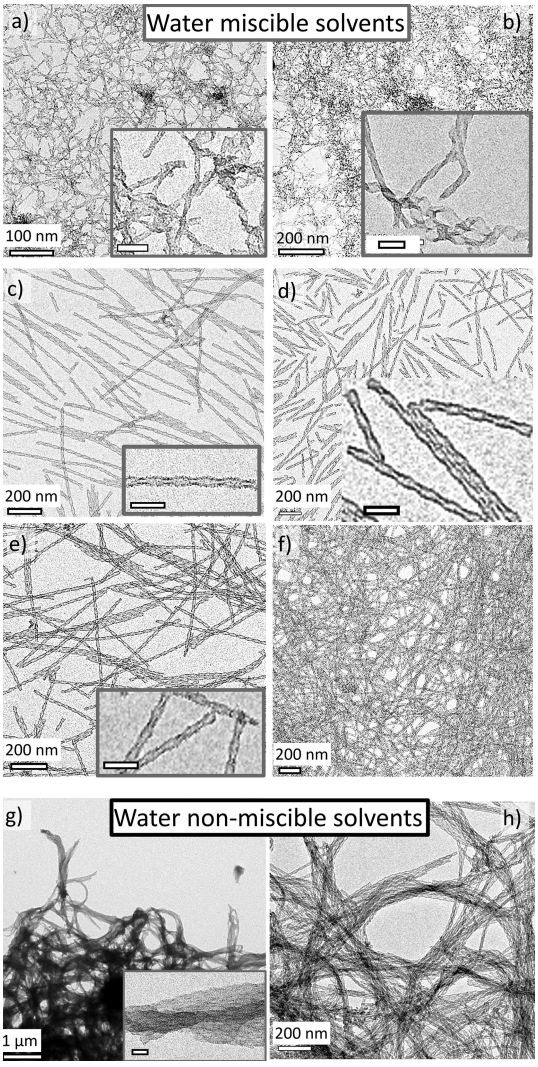

Figure 2. TEM images of silica twisted ribbons submitted to sonication in various solvents: (a) water, water-miscible solvents such as (b) ethanol, (c) DMSO, (d) DMF, (e) pyridine, and (f) acetonitrile, and water-immiscible solvent such as (g) hexane and (h) toluene. Bars in insets: 50 nm.

or in trifluoroethanol (TFE) (see Figure 3), much more clearly fragmented silica fibers with well-preserved chiral fine structure are dispersed in suspension. Interestingly, the fibers were relatively disentangled in acetonitrile (decreased density of knots) but not fragmented (Figure 2f). This is probably due to the low viscosity of acetonitrile as it will be developed later in this article. In solvents which are not miscible with water such as hexane or toluene, silica fibers form aggregates with close-packed bundles. With this method, based on centrifugation and redispersion, there are still water molecules adsorbed on the silica surface which cannot be totally removed. This water layer seems to act as a glue between the fibers, leading to the oriented aggregation in bundles.

Effect of Sonication Power. We then evaluated the effect of sonication power, at fixed silica fiber concentration (1 mg/mL), volume (2 mL), and sonication time

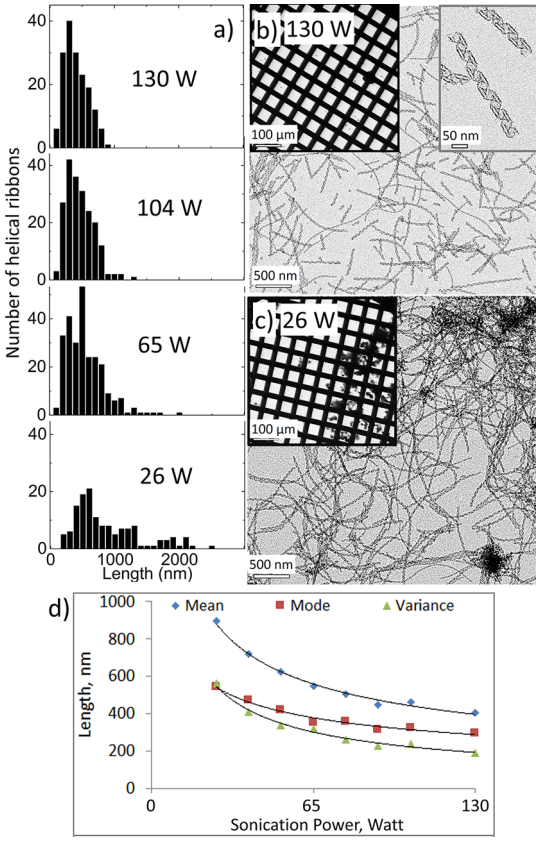

Figure 3. (a) Size distribution of more than 150 helical ribbons sonicated in TFE as a function of the power of the sonication. TEM images of helices after the sonication at (b) 130 W and (c) 26 W. Insets are the low-magnification images, and another inset at high magnification for 130 W. (d) Distribution of helices' length is fitted with a log-normal law and analyzed by Kolmagorov−Smirnov algorithm showing the decrease in the mean, mode, and variance values with increasing sonication power.

(15 min). For this study, TFE was chosen as the solvent in which nanoribbons were sonicated because it was identified as one of the best solvents in the previous section. The sonication power was varied from 0 to 100% of the maximum power (130 W). The size distribution of silica nanohelices submitted to various sonication powers was analyzed by transmission electron microscopy (TEM) as shown in Figure 3. The low-magnification TEM pictures (Figure 3b,c insets) show that, at 26 W, the helices are still strongly aggregated, whereas at 130 W, the helices are well-dispersed and no aggregation is observed. At a higher magnification, we see that the helices are much shorter at 130 W than at 26 W while preserving the well-defined helical morphology (Figure 3b,c). This indicates that in TFE it is possible to induce a scission of the silica helices and to disperse them in solvent without damaging the chiral structure.

To quantify this effect, we measured the silica helices' length as a function of the sonication power. Only the dispersed helices were taken into account as it is not possible to measure the length of the entangled ones. The length of more than 150 helices was measured for each sonication sample to obtain a length distribution with a sufficient precision (Figure 3a). We can clearly see that the higher the sonication power, the lower the maximum length, narrower the length distribution, and lower the mode value (most frequent value) of the distribution of the resulting helices. At 26 W, we observed helices with the length ranging from 200 to 2500 nm, whereas at 65 W, most of the helices were shorter than 1100 nm. At 104 W, most of the helices had lengths between 200 and 800 nm with the most frequently observed length of 400 nm. For 130 W, all the measured helices were shorter than 1000 nm, whereas their overall length distribution was similar to the one observed for 104 W. The data were treated by Kolmagorov−Smirnov algorithm using a log-normal distribution, and a clear decrease in the mean, mode, and variance values with increasing sonication power was observed (Figure 3d). The variance decreases from more than 500 nm for the helices submitted to 26 W sonication to less than 200 nm for those submitted to 130 W sonication. The mode value was also decreased from 900 to 400 nm.

These results show that the sonication power is very important for disentanglment, fragmentation, and suspension of silica fibers in solvents. The higher the sonication power, the lower is the polydispersity of the resulting fibers. In terms of morphologies and sizes of the helices, such as helical pitches and ribbon widths, they do not show notable variation before and after the fragmentation. When combined with the results of solvent variation in the previous section, it is interesting to note that the effect of sonication is observed (i) on the length (fragmentation) while their shapes are not affected and (ii) on their shapes "destroyed" while the length does not change depending on the solvent and sonication power.

Effect of Drying and pH. With the increasing demand for the integration of Green Chemistry, the production of materials with limited use of hazardous substances, more benign to the environment, has become one of the priorities. In this context, water, being environmentally sustainable, is an attractive alternative to organic solvents. Meanwhile, as shown above, the direct fragmentation of silica helices in water does not work well since the cavitation effect in water drastically damages the chiral structures. In order to make them more robust against the cavitation effect during the sonication in water, we have developed a procedure called "dry method" as opposed to the previous wet one, including a freeze-drying pretreatment, in order to obtain silica walls with more consolidated structures. Freeze-drying reinforces the silica wall as it induces the dehydration and reorganization of the silica and leads to more dense structures,[54] without causing the collapse of the network. Concretely, the silica helical and twisted nanoribbons are washed thoroughly with ethanol just after the synthesis to remove the unreacted

TEOS and organic templates and are then washed with water and freeze-dried. The white powder obtained can then be dispersed in different solvents and treated by sonication. The sonication of the suspension in water resulted in fragmented silica helices which are well-calibrated in length with a well-preserved structure (Figure 4). The local chiral structures of helices obtained with this method were well-conserved regardless of the solvents, compared to the "wet method" with which helices were destroyed after sonication in some of the solvents such as water or ethanol. This process also shows the advantage over the wet method because it allows easy quantification of silica before dispersing them in the solvent by weighing the powder when dry. As also observed for the wet method, the dispersibility of these dried helices also depended strongly on the nature of the solvents. In some solvents, they were well-dispersed and the suspension was transparent, whereas in others, they were strongly aggregated, which led to precipitation. The "good" solvents were mostly the same as they were for wet method (*i.e.*, DMSO, pyridine, DMF, and TFE). An important difference was observed between the two methods for water and ethanol. With the wet method, the helices were deformed and aggregated in ethanol, whereas with the dry method, a good dispersion of helices with preserved morphology (helical or twisted ribbons) could be obtained. The aggregation fraction (AF) as calculated and described in the Experimental Section was plotted as a function of solvent parameters such as viscosity, density, molecular weight, and dielectric constants for all the solvents studied (Supporting Information). The results on AF show a good agreement with previous report by Cheng *et al.*[53] on a single-wall carbon nanotube (SWNT); that is, the aggregation fraction decreases with increasing viscosity, density, as well as molecular weight, suggesting that the mechanisms of scission of both fibers are similar as that reported for SWNTs. As they have described, it can be suggested that it requires a higher force and sonication intensity to create cavitation in more viscous liquids; once the cavitation bubbles are created, the temperature and pressure effect resulting from the bubble collapse will be greater, with more efficient fragmentation of the helices.

In the solvents nonmiscible with water such as hexane or toluene, silica fibers were totally aggregated as expected from their lipophobic and hydrophilic nature and due to strong hydrogen bonds which reinforce the cohesion between the silica surfaces in these solvents.

Attempts of dispersion in Milli-Q water at pH 5.5 (typical pH when silica helices are dispersed in Milli-Q water after solvent exchange) led to a strong aggregation. It however is revealed to be strongly dependent on the pH of water. Indeed, because the silica surface

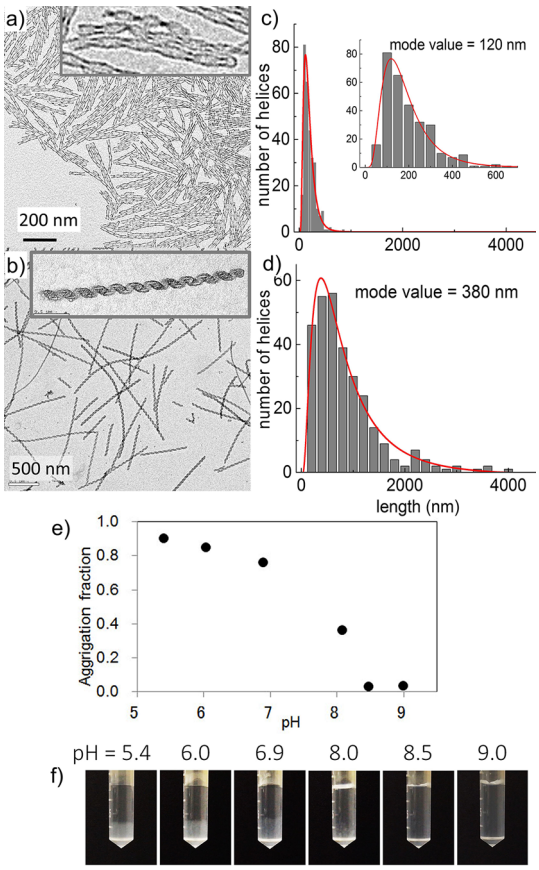

Figure 4. (a) Twisted and (b) helical ribbons made by dry method and redispersed in water at pH 8.5 with concentration of 5 mg/mL for twisted ribbons and 1.25 mg/mL for helical ones. The morphologies of the ribbons are well-preserved, and they are fully dispersed without aggregation. Size distribution of (c) twisted and (d) helical ribbons made by the dry method (on more than 200 helices). (e) Aggregation fraction of the sonicated twisted ribbons in water as a function of pH. (f) Silica helices dispersed in water with various pH values.

charge varies with the pH, the dispersion of the silica colloids is strongly modified accordingly; that is, the decrease of the pH induces protonation of the negatively charged surface oxygen and the conversion to OH. As a consequence, there is a strong decrease of the overall surface charge and an increase of affinity of the helices with their neighbors due to the hydrogen bonding and the van der Waals interactions, leading to their aggregation.

To evaluate the dispersibility of silica helices in water, we adjusted the pH to different values from 5.5 to 9 with sodium hydroxide 0.1 N solution and proceeded with the sonication at 130 W, for 15 min (Figure 4).

As it is well-illustrated in Figure 4a,b,e,f, no aggregation is observed for pH higher than 8 after the sonication. The negative charge of the silica surface in this pH range stabilizes the colloidal suspension by electrostatic repulsions. For pH below 8, the helices show strong aggregation. Again, the optimization of

the choice of the parameters is of great importance. We observed that the optimal concentration of the twisted ribbons for the sonication process is 5 mg/mL, whereas for the helical ribbons, the best results were obtained for 1.25 mg/mL. For higher concentration of helical ribbons, the helices are indeed very short but some of them are broken into small pieces which induce aggregation (Supporting Information). The size distribution of both twisted and helical ribbons cut in the optimal conditions were analyzed and are shown in Figures 4c,d. The results obtained with the helical ribbons are similar to those obtained with the wet method as the diagram shows a mode value of 380 nm and a long tail showing that some helices remain very long (variance is 880 nm). On the contrary, the sonication of the twisted ribbons induces short ribbons as the mode value is 120 nm, and the length shows a real monodispersity with a variance of 68 nm. This monodispersity is crucial for potential applications such as the hierarchical organization of the fibers as alignment or compact stacking.

CONCLUSION

We have optimized a process of quick transcription of silica fibers with controlled chirality (helical or twisted ribbons) based on sol−gel chemistry using organic self-assembly as a template. By acidifying the TEOS solution from pH 6.0 to 3.8 using chiral acid, tartaric acid, which allows the control at the same time of the supramolecular chirality of the template, the prehydrolysis was strongly accelerated, and it was possible to obtain helical silica nanoribbons within 3 days instead of 23 days. Twisted silica nanoribbons were obtained after 1 day instead of 7 days compared to our previous report.

For the purpose of application, it is crucial to control not only the local chiral structures of these fibers (diameter, pitch) but also their length in order to obtain homogeneous suspension of these colloidal nano-objects. We demonstrated that the sonication method inspired by the report on the carbon nanotubes *can be extended* to inorganic metal oxide structures such as silica fiber systems to disentangle, fragment them, and get helical and twisted silica ribbons with well-preserved nanometric morphologies of several hundreds of nanometers in length. We have shown that the power of sonication is an important parameter: for a *maximum* power of 130 W, the higher the power of the sonication, the narrower the distribution of the fragmented helices, and the better the dispersion. The nature of the solvent is also a crucial parameter. Solvents with high viscosity, high molecular weight, high density, and low dielectric constant such as TFE, DMSO, pyridine, or DMF turned out to be the best ones for obtaining good dispersion of well-fragmented helices with retained chiral morphology. The good agreement between these results with the previous report on carbon nanotubes indicates that this approach reported on SWNTs can be extended to metal oxide nanostructures, that the mechanism of fragmentation and dispersion of the nano-objects follows the similar rule, and the debundling and scission result from the cavitation collapse which is more efficient in viscous liquid than in less viscous liquid.

Freeze-drying of the helices clearly consolidated the Si−O−Si bonds. The sonication of helices in water or in ethanol directly after the transcription destroyed the local chiral structures, whereas the helices which were freeze-dried first and then dispersed in these solvents preserved their local chiral structure after sonication. In the case of water, the pH has a crucial effect on the dispersibility, and homogeneous dispersions of helices were obtained only for pH above 8. The application of sonication on the nanometric chiral fibrous structures for which the local structures are consolidated by freeze-drying showed homogeneous colloidal suspension of individualized and size-controlled chiral nanometric silica fibers. This study describes for the first time scaled-up synthesis and formation of stable chiral colloidal homogeneous suspensions, based on self-organized chiral elongated structures, extremely promising for numerous applications.

EXPERIMENTAL SECTION

Gemini Tartrate. The procedure for bromide to tartrate ion exchange for the synthesis of 16-2-16 tartrate was optimized from the procedure described previously[42] to achieve exact stoichiometry. First, 16-2-16 acetate was synthesized from 16-2-16 Br by ion exchange reaction with silver acetate as previously reported.[55] Then the acetate was replaced with tartrate by mixing the solution of 16-2-16 acetate in (typically 100 mg) with the solution of 2 equiv of corresponding tartaric acid (both 10 mL of MeOH/acetone (1:9) mixture). As tartaric acid solution was added to the solution of 16-2-16 Ac under stirring, a white precipitate of 16-2-16 tartrate was formed. It was filtered and washed with several portions of acetone. The excess of tartaric acid was washed away with cold water (1 °C).

Organic Gels. The 16-2-16 tartrate is solubilized in Milli-Q water (typically, 3.6 mg of 16-2-16 L-tartrate powder is dissolved into 5 mL of Milli-Q water, for a concentration of 1 mM 16-2-16 tartrate), and the solution is heated at 60 °C (above the Krafft temperature which is 43 °C). At the concentration of 1 mM, twisted ribbons were observed after 1 h at 20 °C and helical ribbons were observed after 1 day. The morphology of self-assembly was monitored with TEM.

Inorganic Transcription. TEOS (500 μL) was added to the 10 mL of 0.1 mM aqueous solution of L-tartaric acid (pH 3.8) and prehydrolyzed at 20 °C by stirring on the roller-mixer for 7 h. In parallel, a solution of 1 mM 16-2-16 gemini surfactant with L-tartrate counterion is aged between 2 h and 2 days for the formation of twisted or helical nanoribbons, respectively. Equal volumes of prehydrolyzed TEOS in 0.1 mM aqueous solution of L-tartaric acid and organic gels are mixed (typically, 2 mL of each) and stirred at 20 °C with a roller-mixer overnight. The use of roller-mixer is crucial because it optimizes the contact of

prehydrolyzed TEOS and organic fibers. Once the transcription is completed, the mixture is washed thoroughly with ethanol to eliminate the excess of TEOS (washing four times with absolute ethanol by centrifugation (5 min, 2000*g*) and redispersing in ethanol). Finally, the suspension of silica fibers is stored in pure ethanol. With this procedure, we obtained on average 0.6 mg of silica helical ribbons and 1.1 mg of silica twisted ribbons from 0.36 mg of gemini.

Sonication. A high intensity ultrasonic processor (Vibra cell 75186) equipped with 6 mm microtip with variable power was used (maximum power, 130 W). A 20 kHz pulse mode was used for the dispersion and fragmentation of silica nanohelices and twisted nanoribbons. For the study of the effect of the sonication power and nature of the solvent on the efficiency of scission and dispersion of the silica nano-objects with the wet method, the rest of the experimental parameters were kept constant: sample concentration (1 mg/mL), volume (2 mL), sonication time (15 min with pulses of 1 s separated by 1 s pauses). Samples were cooled in an ice bath during the sonication process in order to avoid solvent evaporation and increasing of the sample temperature which could influence the sonication effect. Two groups of solvents were used in this study: (1) water-miscible solvents: water, ethanol, TFE, DMSO, DMF, acetonitrile, pyridine; (2) water-immiscible solvents: hexane and toluene. Sonication after freeze-drying pretreatment dry method: the silica helices' dispersion in ethanol was washed four times with Milli-Q water using centrifugation. The residue was freeze-dried for 1 day to give a white powder (temperature and vacuum) because they influence the final result of consolidation. Two milliliters of Milli-Q water was added to *x* milligrams of the silica powder ($x = 10$ for twisted ribbons and 2.5 for helical ribbons), and this mixture was sonicated for 15 min in the ice bath. The pH of this mixture was adjusted with 0.1 N aqueous NaOH and sonicated for another 15 min in the ice bath.

Aggregation Fraction. One milliliter of the pH-adjusted mixture (conc = 5 mg/mL for twisted ribbons) was separated into the precipitate part and supernatant part by centrifugation at 1000 rpm (192*g*) for 2 min, and the supernatant was removed. Then the pellet and the supernatant were freeze-dried. Weights of the supernatant ($W_{supernatant}$) and the precipitate ($W_{precipitate}$) were measured, and the aggregation fractions were calculated according to eq 1.

$$\text{aggregation fraction} = \frac{\text{aggregation part}}{\text{total weight}} = \frac{W_{precipitate}}{W_{precipitate} + W_{supernatant}} \quad (1)$$

Characterization of Silica Nanohelices. After each step of the synthesis, samples were characterized by TEM. The 400 mesh carbon-coated copper grids were used for the TEM. For the observation of the samples prepared in water, hydrophilic grids were prepared. For this, carbon-coated copper grids were treated in BioForce Nanosciences UV/ozone ProCleaner 220 for 10 min. For the sample preparation, 5 μL of the silica suspension was drop-casted onto the grid and blotted after 1 min. Samples were dried in air.

TEM observations were performed using a Philips EM 120 electron microscope operating at 120 kV, and the images were collected by 2k × 2k Gatan ssCCD camera.

The measurement of the ribbon length was done with the ImageJ software, and the analysis of the length distribution was performed using a log-normal low and confirmed with the Kolmagorov–Smirnov algorithm. From the histograms of the silica fiber length after the sonication, we assumed log-normal distribution of this value. If some value X is log-normally distributed, then $Y = \ln(X)$ has a normal distribution. Therefore, we calculated natural logarithm of the silica fiber lengths and subjected obtained data to the normality test using Kolmagorov–Smirnov algorithm in OriginPro 9 software. With the significance level of 0.05, the test confirms the normal distribution of the natural logarithm of the silica fiber lengths and so the log-normal distribution of the lengths themselves. Mean value (μ) and standard deviation (σ) of normal distribution were obtained as parameters from the normality test. These parameters were used to calculate the mean and mode values as well as variation of the silica fibers length distribution (log-normal) according to the follow equations:

$$\text{mode} = e^{\mu - \sigma^2}$$

$$\text{mean} = e^{\mu + \sigma^2/2}$$

$$\text{variance} = (e^{\sigma^2} - 1)e^{2\mu + \sigma^2}$$

Typically, the square root of the variance is used to describe how far a set of values is spread out. The method described above was applied to the data obtained for various sonication powers. The values of mode, mean, and square root of variance showed power-law dependence on the sonication power.

Conflict of Interest: The authors declare no competing financial interest.

Acknowledgment. The authors want to gratefully acknowledge for the financial support by the "Agence Nationale de la Recherche" Grant No. ANR-10-BLAN-0813 (NANOSPRINGS), Strategic Young Researcher Overseas Visits Program for Accelerating Brain Circulation, Japan Society for the Promotion of Science, the LabEx AMADEus (ANR-10-LABX-42) in the framework of IdEx Bordeaux (ANR-10-IDEX-03-02), *i.e.*, the Investissements d'Avenir programme of the French government managed by the Agence Nationale de la Recherche and ERASMUS MUNDUS grant awarded by the European Commission, International Doctoral School in Functional Materials for Energy, Information Technology, and Health–IDS FunMat.

Supporting Information Available: Figures S1–S4. This material is available free of charge *via* the Internet at http://pubs.acs.org.

REFERENCES AND NOTES

1. Xia, Y.; Yang, P.; Sun, Y.; Wu, Y.; Mayers, B.; Gates, B.; Yin, Y.; Kim, F.; Yan, H. One-Dimensional Nanostructures: Synthesis, Characterization, and Applications. *Adv. Mater.* **2003**, *15*, 353–389.
2. Mann, S. Self-Assembly and Transformation of Hybrid Nano-objects and Nanostructures under Equilibrium and Non-equilibrium Conditions. *Nat. Mater.* **2009**, *8*, 781–792.
3. Shimizu, T.; Masuda, M.; Minamikawa, H. Supramolecular Nanotube Architectures Based on Amphiphilic Molecules. *Chem. Rev.* **2005**, *105*, 1401–1444.
4. Burda, C.; Chen, X.; Narayanan, R.; El-Sayed, M. A. Chemistry and Properties of Nanocrystals of Different Shapes. *Chem. Rev.* **2005**, *105*, 1025–1102.
5. Peng, L.; Ran, L.; Mortensen, N. A. Achieving Anisotropy in Metamaterials Made of Dielectric Cylindrical Rods. *Appl. Phys. Lett.* **2010**, *96*, 241108.
6. Pouget, E.; Dujardin, E.; Cavalier, A.; Moreac, A.; Valery, C.; Marchi-Artzner, V.; Weiss, T.; Renault, A.; Paternostre, M.; Artzner, F. Hierarchical Architectures by Synergy between Dynamical Template Self-Assembly and Biomineralization. *Nat. Mater.* **2007**, *6*, 434–439.
7. van Blaaderen, A. Materials Science: Colloids Get Complex. *Nature* **2006**, *439*, 545–546.
8. Kuijk, A.; van Blaaderen, A.; Imhof, A. Synthesis of Monodisperse, Rodlike Silica Colloids with Tunable Aspect Ratio. *J. Am. Chem. Soc.* **2011**, *133*, 2346–2349.
9. Srivastava, S.; Kotov, N. A. Nanoparticle Assembly for 1D and 2D Ordered Structures. *Soft Matter* **2009**, *5*, 1146–1156.
10. Glotzer, S. C.; Solomon, M. J. Anisotropy of Building Blocks and Their Assembly into Complex Structures. *Nat. Mater.* **2007**, *6*, 557–562.
11. Pouget, E.; Grelet, E. Dispersions of Monodisperse Hybrid Rod-like Particles by Mineralization of Filamentous Viruses. *Langmuir* **2013**, *29*, 8010–8016.
12. Wang, Y.; Xu, J.; Wang, Y.; Chen, H. Emerging Chirality in Nanoscience. *Chem. Soc. Rev.* **2013**, *42*, 2930–2962.

13. Li, Q.; Lu, G. Controlled Synthesis and Photocatalytic Investigation of Different-Shaped One-Dimensional Titanic Acid Nanomaterials. *J. Power Sources* **2008**, *185*, 577–583.
14. Chen, X.; Mao, S. S. Titanium Dioxide Nanomaterials: Synthesis, Properties, Modifications, and Applications. *Chem. Rev.* **2007**, *107*, 2891–2959.
15. Polavarapu, L.; Xu, Q.-H. Water-Soluble Conjugated Polymer-Induced Self-Assembly of Gold Nanoparticles and Its Application to SERS. *Langmuir* **2008**, *24*, 10608–10611.
16. Li, Z.; Zhu, Z.; Liu, W.; Zhou, Y.; Han, B.; Gao, Y.; Tang, Z. Reversible Plasmonic Circular Dichroism of Au Nanorod and DNA Assemblies. *J. Am. Chem. Soc.* **2012**, *134*, 3322–3325.
17. Liu, W.; Zhu, Z.; Deng, K.; Li, Z.; Zhou, Y.; Qiu, H.; Gao, Y.; Che, S.; Tang, Z. Gold Nanorod@Chiral Mesoporous Silica Core−Shell Nanoparticles with Unique Optical Properties. *J. Am. Chem. Soc.* **2013**, *135*, 9659–9664.
18. Wang, Z. L. The New Field of Nanopiezotronics. *Mater. Today* **2007**, *10*, 20–28.
19. Dickerson, M. B.; Sandhage, K. H.; Naik, R. R. Protein- and Peptide-Directed Syntheses of Inorganic Materials. *Chem. Rev.* **2008**, *108*, 4935–4978.
20. Kobayashi, S.; Hamasaki, N.; Suzuki, M.; Kimura, M.; Shirai, H.; Hanabusa, K. Preparation of Helical Transition-Metal Oxide Tubes Using Organogelators as Structure-Directing Agents. *J. Am. Chem. Soc.* **2002**, *124*, 6550–6551.
21. Bae, C.; Yoo, H.; Kim, S.; Lee, K.; Kim, J.; Sung, M. M.; Shin, H. Template-Directed Synthesis of Oxide Nanotubes: Fabrication, Characterization, and Applications. *Chem. Mater.* **2008**, *20*, 756–767.
22. Delclos, T.; Aimé, C.; Pouget, E.; Brizard, A.; Huc, I.; Delville, M.-H.; Oda, R. Individualized Silica Nanohelices and Nanotubes: Tuning Inorganic Nanostructures Using Lipidic Self-Assemblies. *Nano Lett.* **2008**, *8*, 1929–1935.
23. Qiu, H.; Che, S. Chiral Mesoporous Silica: Chiral Construction and Imprinting *via* Cooperative Self-Assembly of Amphiphiles and Silica Precursors. *Chem. Soc. Rev.* **2011**, *40*, 1259–1268.
24. Lin, Y.; Qiao, Y.; Gao, C.; Tang, P.; Liu, Y.; Li, Z.; Yan, Y.; Huang, J. Tunable One-Dimensional Helical Nanostructures: From Supramolecular Self-Assemblies to Silica Nanomaterials. *Chem. Mater.* **2010**, *22*, 6711–6717.
25. Qiao, Y.; Wang, Y.; Yang, Z.; Lin, Y.; Huang, J. Self-Templating of Metal-Driven Supramolecular Self-Assembly: A General Approach toward 1D Inorganic Nanotubes. *Chem. Mater.* **2011**, *23*, 1182–1187.
26. Jin, C.; Qiu, H.; Han, L.; Shu, M.; Che, S. DNA Transcription into Diverse Porous Silicas by a Co-structure Directing Route: Chiral, Ring and Ordered Nanochannel Arrays. *Chem. Commun.* **2009**, 3407–3409.
27. Liu, S.; Duan, Y.; Feng, X.; Yang, J.; Che, S. Synthesis of Enantiopure Carbonaceous Nanotubes with Optical Activity. *Angew. Chem., Int. Ed.* **2013**, *52*, 6858–6862.
28. Jung, J. H.; Ono, Y.; Hanabusa, K.; Shinkai, S. Creation of Both Right-Handed and Left-Handed Silica Structures by Sol−Gel Transcription of Organogel Fibers Composed of Chiral Diaminocyclohexane Derivatives. *J. Am. Chem. Soc.* **2000**, *122*, 5008–5009.
29. Han, T. H.; Oh, J. K.; Park, J. S.; Kwon, S.-H.; Kim, S.-W.; Kim, S. O. Highly Entangled Hollow TiO_2 Nanoribbons Templating Diphenylalanine Assembly. *J. Mater. Chem.* **2009**, *19*, 3512–3516.
30. Li, X.; Wu, Y.; Li, Y. Surfactant-Assisted Synthesis of Helical Silica. *Inorg. Chim. Acta* **2007**, *360*, 241–245.
31. Kim, W.-J.; Yang, S.-M. Helical Mesostructured Tubules from Taylor Vortex-Assisted Surfactant Templates. *Adv. Mater.* **2001**, *13*, 1191–1195.
32. a) Grzelczak, M.; Vermant, J.; Furst, E. M.; Liz-Marzán, L. M. Directed Self-Assembly of Nanoparticles. *ACS Nano* **2010**, *4*, 3591–3605. b) Liu, K.; Zhao, N.; Kumacheva, E. Self-Assembly of Inorganic Nanorods. *Chem. Soc. Rev.* **2011**, *40*, 656–671. c) Min, Y.; Akbulut, M.; Kristiansen, K.; Golan, Y.; Israelachvili, J. The Role of Interparticle and External Forces in Nanoparticle Assembly. *Nat. Mater.* **2008**, *7*, 527–538. d) Nie, Z.; Petukhova, A.; Kumacheva, E. Properties and Emerging Applications of Self-Assembled Structures Made from Inorganic Nanoparticles. *Nat. Nanotechnol.* **2010**, *5*, 15–25.
33. Yang, S.; Zhao, L.; Yu, C.; Zhou, X.; Tang, J.; Yuan, P.; Chen, D.; Zhao, D. On the Origin of Helical Mesostructures. *J. Am. Chem. Soc.* **2006**, *128*, 10460–10466.
34. Jin, H.; Liu, Z.; Ohsuna, T.; Terasaki, O.; Inoue, Y.; Sakamoto, K.; Nakanishi, T.; Ariga, K.; Che, S. Control of Morphology and Helicity of Chiral Mesoporous Silica. *Adv. Mater.* **2006**, *18*, 593–596.
35. Dogic, Z.; Fraden, S. Ordered Phases of Filamentous Viruses. *Curr. Opin. Colloid Interface Sci.* **2006**, *11*, 47–55.
36. Grelet, E. Hexagonal Order in Crystalline and Columnar Phases of Hard Rods. *Phys. Rev. Lett.* **2008**, *100*, 168301.
37. Gregory, J.; Holmes, K. C. Methods of Preparing Orientated Tobacco Mosaic Virus Sols for X-ray Diffraction. *J. Mol. Biol.* **1965**, *13*, 796–IN15.
38. Bernal, J. D.; Fankuchen, I. X-ray and Crystallographic Studies of Plant Virus Preparations. *J. Gen. Physiol.* **1941**, *25*, 111–146.
39. Fowler, C. E.; Shenton, W.; Stubbs, G.; Mann, S. Tobacco Mosaic Virus Liquid Crystals as Templates for the Interior Design of Silica Mesophases and Nanoparticles. *Adv. Mater.* **2001**, *13*, 1266–1269.
40. Menger, F. M.; Keiper, J. S. Gemini Surfactants. *Angew. Chem., Int. Ed.* **2000**, *39*, 1906–1920.
41. Zana, R.; Xia, J. *Gemini Surfactants: Synthesis, Interfacial and Solution-Phase Behavior, and Applications*; Marcel Dekker: New York, 2004; Vol. 117, p 331.
42. Brizard, A.; Aime, C.; Labrot, T.; Huc, I.; Berthier, D.; Artzner, F.; Desbat, B.; Oda, R. Counterion, Temperature, and Time Modulation of Nanometric Chiral Ribbons from Gemini-Tartrate Amphiphiles. *J. Am. Chem. Soc.* **2007**, *129*, 3754–3762.
43. Oda, R.; Huc, I.; Candau, S. J. Gemini Surfactants as New, Low Molecular Weight Gelators of Organic Solvents and Water. *Angew. Chem., Int. Ed.* **1998**, *37*, 2689–2691.
44. Oda, R.; Huc, I.; Schmutz, M.; Candau, S. J.; MacKintosh, F. C. Tuning Bilayer Twist Using Chiral Counterions. *Nature* **1999**, *399*, 566–569.
45. Brizard, A.; Berthier, D.; Aime, C.; Buffeteau, T.; Cavagnat, D.; Ducasse, L.; Huc, I.; Oda, R. Molecular and Supramolecular Chirality in Gemini-Tartrate Amphiphiles Studied by Electronic and Vibrational Circular Dichroisms. *Chirality* **2009**, *21*, E153–E162.
46. Sugiyasu, K.; Tamaru, S.; Takeuchi, M.; Berthier, D.; Huc, I.; Oda, R.; Shinkai, S. Double Helical Silica Fibrils by Sol−Gel Transcription of Chiral Aggregates of Gemini Surfactants. *Chem. Commun.* **2002**, 1212–1213.
47. Tamoto, R.; Lecomte, S.; Si, S.; Moldovan, S.; Ersen, O.; Delville, M.-H.; Oda, R. Gold Nanoparticle Deposition on Silica Nanohelices: A New Controllable 3D Substrate in Aqueous Suspension for Optical Sensing. *J. Phys. Chem. C* **2012**, *116*, 23143–23152.
48. Das, R. K.; Zouani, O. F.; Labrugère, C.; Oda, R.; Durrieu, M.-C. Influence of Nanohelical Shape and Periodicity on Stem Cell Fate. *ACS Nano* **2013**, *7*, 3351–3361.
49. Hennrich, F.; Krupke, R.; Arnold, K.; Rojas Stütz, J. A.; Lebedkin, S.; Koch, T.; Schimmel, T.; Kappes, M. M. The Mechanism of Cavitation-Induced Scission of Single-Walled Carbon Nanotubes. *J. Phys. Chem. B* **2007**, *111*, 1932–1937.
50. Lucas, A.; Zakri, C.; Maugey, M.; Pasquali, M.; van der Schoot, P.; Poulin, P. Kinetics of Nanotube and Microfiber Scission under Sonication. *J. Phys. Chem. C* **2009**, *113*, 20599–20605.
51. Warakulwit, C.; Majimel, J.; Delville, M.-H.; Garrigue, P.; Limtrakul, J.; Kuhn, A. Controlled Purification, Solubilisation and Cutting of Carbon Nanotubes Using Phosphomolybdic Acid. *J. Mater. Chem.* **2008**, *18*, 4056–4061.
52. Brizard, A.; Ahmad, R. K.; Oda, R. Control of Nano-Micrometric Twist and Helical Ribbon Formation with Gemini-Oligoalanine *via* Interpeptidic β-Sheet Structure Formation. *Chem. Commun.* **2007**, 2275–2277.
53. Cheng, Q.; Debnath, S.; Gregan, E.; Byrne, H. J. Ultrasound-Assisted SWNTs Dispersion: Effects of Sonication Parameters and Solvent Properties. *J. Phys. Chem. C* **2010**, *114*, 8821–8827.

54. Iler, R. K. *The Chemistry of Silica: Solubility, Polymerization, Colloid and Surface Properties and Biochemistry of Silica*; Wiley-Interscience: New York, 1979.
55. Manet, S.; Karpichev, Y.; Bassani, D.; Kiagus-Ahmad, R.; Oda, R. Counteranion Effect on Micellization of Cationic Gemini Surfactants 14-2-14: Hofmeister and Other Counterions. *Langmuir* **2010**, *26*, 10645–10656.